

**EXPERIMENTAL DETERMINATION OF MODE
SHAPES FOR A LIGHTLY DAMPED
STRUCTURE WITH UNKNOWN
TRANSIENT EXCITATION**

By

PETER MARTIN

Bachelor of Science

Harvey Mudd College

Claremont, California

1991

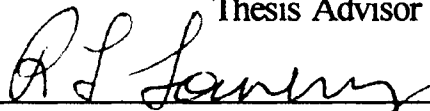
**Submitted to the Faculty of the
Graduate College of the
Oklahoma State University
in partial fulfillment of
the requirements for
the Degree of
MASTER OF SCIENCE
May, 1994**

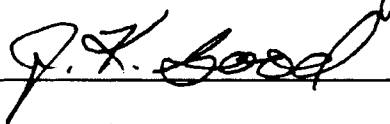
EXPERIMENTAL DETERMINATION OF MODE
SHAPES FOR A LIGHTLY DAMPED
STRUCTURE WITH UNKNOWN
TRANSIENT EXCITATION

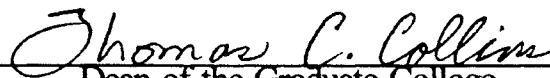
Thesis Approved:



Thesis Advisor







Dean of the Graduate College

PREFACE

I desired to find the mode shapes of a structure without measuring the input excitation force. The eventual application for this research will be in the determination of the flutter modes of a web. The web, being very light, would have its mass significantly affected by the attachment of a vibration transducer and cannot be excited in any measurable fashion by a calibrated impact hammer. The vibration of the web can, however, be measured by laser-Doppler velocimeters that will detect the velocity of select points on the web without the need to attach anything to the web at all. The question before my research was: are time histories of the motion of a structure at select points along its surface enough information to develop discrete mode shapes, without knowing the excitation? In order to answer this question, I chose a simple structure to work with--one whose mode shapes can be calculated analytically: a cantilever beam. I measured the vibration of the beam using two very light accelerometers that had negligible effect on the beam's mass. Using one accelerometer as a stationary reference, frequency response functions between it and a roving accelerometer were determined at several points along the beam's length. Using the peak picking technique, mode shapes were determined from these functions. These shapes are almost identical to the theoretical mode shapes calculated for my beam. Therefore, I achieved my goal because I never measured the type or amount of force I was using to set the beam in motion--I tapped it with my finger.

I wish to express my sincere gratitude to the individuals who assisted me in this project and during my coursework at Oklahoma State University. In particular, I wish to thank my major advisor, Dr. Peter M. Moretti, for his intelligent guidance. I am also grateful to the other committee members, Dr. R.L. Lowery and Dr. J.K. Good, for their invaluable assistance during the course of this work, and to Dr. Timothy M. Minahen, who initially served as my major advisor.

Special thanks are due to the staff at the Mechanical and Aerospace Engineering Research Lab. I would also like to express my gratitude to Dr. Young Bae Chang, a post-doctoral candidate, for his assistance in the use of the spectrum analyzer used to obtain frequency response functions.

The help of Mike Mason at Zonic Corporation in Milford, Ohio is also sincerely appreciated. I don't know how I could have ever mastered the use of the modal analyzer --used to make preliminary measurements--without him.

Special thanks are due to my friends, Ashraf Nimer, Yves Dallenbach, and Sani Daher, for helping me type out this thesis.

TABLE OF CONTENTS

Chapter	Page
I. INTRODUCTION.1
Background1
The Experiment3
The Frequency Response Function.6
II. FUNCTION OF A MODAL ANALYZER.	10
Spectral Analysis.	10
Parameter Estimation	11
III. THEORETICAL PREDICTIONS	14
Natural Frequencies.	14
Mode Shapes.	15
IV. RESULTS	16
Preliminaries.	16
Finding the Mode Shapes.	19
V. VERIFICATION.	28
Time Response at Free End.	28
Modal Assurance Criterion.	33
VI. CONCLUSION.	35
VII. SUGGESTIONS FOR FURTHER RESEARCH.	38
WORKS CITED.	39
APPENDIX - OBTAINING A MODAL MODEL WITHOUT MEASURING THE STRUCTURE'S EXCITATION: AN UNDERDETERMINED SYSTEM.	40

LIST OF TABLES

Table	Page
I. Ranges of Measured Natural Frequencies.19
II. Measured vs. Theoretical Mode Shapes.27

LIST OF FIGURES

Figure	Page
1. Experimental Set-up.	5
2. A System to be Analyzed Spectrally	7
3. Typical Time Signal from an Accelerometer (traced by hand from screen)17
4. FFT Magnitude and Phase Plots for Signal in Figure 3 on Page 17 (traced by hand from screen).18
5. Typical FRF Magnitude and Phase Plots (traced by hand from screen)21
6. Measured vs. Theoretical for First Mode.22
7. Measured vs. Theoretical for Second Mode23
8. Measured vs. Theoretical for Third Mode.24
9. Measured vs. Theoretical for Fourth Mode25
10. Measured vs. Theoretical for Fifth Mode.26
11. Theoretical Acceleration of the Beam's Free End.31
12. Measured Record from Free End Accelerometer (traced by hand from screen)32
13. Simplest Modal Analysis Scenario42

NOMENCLATURE

$A1(s)$	Fourier transform of roving accelerometer's signal
$A2(s)$	Fourier transform of stationary accelerometer's signal
$A1(t)$	time history from roving accelerometer
$A2(t)$	time history from stationary accelerometer
c	damping
δ	unit impulse function
$f(x,t)$	external excitation of the beam
F	force imparted to the structure
FFT	Fast Fourier Transform
FRF	frequency response function
G_{bb}	auto spectral density of time signal b
G_{bc}	cross spectral density of time signals b and c
H_0	the true frequency response of a system
H_1	the most commonly used FRF
$H(s)$	FRF used in the experiment
H_2	an FRF affected by output noise
H_v	a very accurate FRF
k	stiffness
λ_r	the eigenvalues of the characteristic equation

m	mass
$mdof$	multi-degree-of-freedom
$m(t)$	the noise in the output of a system
$n(t)$	the noise in the input signal of a system
Q_r	generalized forces exciting the structure
r	mode number
$*$	the complex conjugate
t	time
$u(t)$	the true input of a system
$V_r(x)$	the mode shapes of the structure
$v(t)$	the true output of a system
ω_r	the natural frequencies of the structure in radians per second
x	the horizontal location on the beam (equal to zero at the clamped end)
$y(t)$	time signal from a measurement point on a simple structure
$y(x,t)$	the vertical displacement of the beam

CHAPTER I

INTRODUCTION

Background

Conventionally, modal analysis of structures is conducted by measuring many frequency response functions. These functions, which resemble transfer functions, have as their input and output the Fourier transforms of records of excitation forces and vibrational response. A typical FRF (frequency response function) will have the Fourier transform of the excitation time history as its input, and the Fourier transform of a vibration transducer's record as its output. The vibration transducer is usually located somewhere on the structure, and may measure acceleration, velocity, or displacement. To obtain the several FRF's required, the excitation (commonly applied and measured with a calibrated impact hammer) can be moved to different locations on the structure while the vibration transducer remains stationary. This procedure ensures that all of the FRF's have the same reference point. Another possibility is to move the transducer to different locations on the structure while always exciting the structure in the same location. The reason an impact hammer is usually used as the excitation is because an impulse (the ideal of the time history obtained with a quick whack from the hammer) transforms into a uniformly flat signal in the frequency domain, which is simple to work with and excites all frequencies of interest. Other excitations such as random or sinusoidal are permissible

and, in some applications, preferable. The time histories are usually recorded with a spectrum analyzer, which has a Fast Fourier Transform (FFT) algorithm programmed into it in order to perform the Fourier transformations of these time histories. Once the structure has been appropriately discretized into points of measurement, and all of the FRF's have been obtained, the natural frequencies of the structure will be known because they occur at the peaks of the Fourier transforms of the vibration time histories as well as at the peaks of the FRF's. This discretization is arbitrary and the number of points of measurement must be chosen wisely by the modal analyst, such that the resulting discrete mode shapes--whose number of relative deflection values is equal to the number of measurement points--will give an accurate representation of the motion of what is actually a continuous system. The FRF's are then compared in order to obtain the mode shapes of the structure, and they can be further processed by a modal analyzer's modal software program in order to obtain the modal model of the structure (i.e., mass, stiffness, and damping matrices).

Such is the norm, but what if it is desired to find the flutter mode shapes of a very light and extremely flexible structure such as a thin plastic web? Such a structure would have its mass greatly affected by the attachment of a vibration transducer, and hence any natural frequencies or mode shapes obtained would be highly suspect to error. Velocity, however, can be measured by laser-Doppler velocimeters, which are not attached to the structure, and therefore do not affect its mass. The question that arises is whether or not velocity measurements will suffice for obtaining mode shapes. This topic will be addressed in the Conclusion. Also, the high degree of damping in a plastic web will create phase shifts in the frequency plots of any vibration signals measured. These phase shifts,

depending on their degree, may make it very difficult to apply certain modal analysis techniques used to acquire mode shapes. This possible difficulty will be addressed in the chapter on suggestions for further research, since it will not present a problem in the experiment conducted for the research discussed in this paper. But what about the excitation? Obtaining an accurate time history of the excitation required to set a web in flutter (likely to be a crosswind) is extremely difficult. And so, the question arises: can mode shapes be acquired without measuring the force used to excite the structure? One way of acquiring mode shapes is to excite the structure at its natural frequencies (sinusoidal excitation), and then record the structure's motion. This motion, since it occurs at a natural frequency, must represent the mode of vibration associated with that frequency. The other modes are not excited unless the excitation is at a frequency other than the natural frequency associated with that mode. Although this technique of obtaining mode shapes is common, its successful application to a highly flexible web is difficult. And so, the real question is: can mode shapes be obtained by exciting the structure at a range of frequencies, and without measuring this excitation? Answering this question is the subject of this thesis. The hypothesis is that mode shapes can, indeed, be found by measuring response, without measuring the excitation.

The Experiment

A simple cantilever beam was chosen as the test structure because its natural frequencies and mode shapes can be determined analytically, and in turn compared to the experimental results. Two very light A353B17 accelerometers were purchased from PCB so as not to significantly affect the mass of the beam. In fact, their combined weight is

approximately 2.2% of the weight of the beam, allowing one to ignore their mass when predicting what the natural frequencies of the beam will be (Laura, Pombo, & Susemihl 1974). Other important specifications are 10 mV/g voltage sensitivity, 1 to 10000 Hz frequency range ($\pm 5\%$), 500g amplitude range, and .01g peak resolution. The accelerometers were powered by 480D06 DC power supplies from PCB for minimal noise in the signals. These signals, $A_1(t)$ and $A_2(t)$, were filtered by a 30 kHz low-pass filter built into the Data Precision 6100 spectrum analyzer, in order to avoid aliasing. Only acceleration time histories will be used to attempt to find the mode shapes of the structure. The question that, hence, arises is whether causality is an issue between the input and output. Conventionally, when a force and a vibration are measured, the vibration is obviously caused by the force and occurs after the force is applied; therefore, measurement of both signals should clearly begin (or be triggered) at the instant the force is applied. With two accelerometers, however, it is uncertain which one should act as the trigger for measurement to begin. It is also uncertain whether or not one needs to know which transducer will be affected by the excitation first. These questions will be answered in the conclusion. The set-up looked like Figure 1 on page 5.

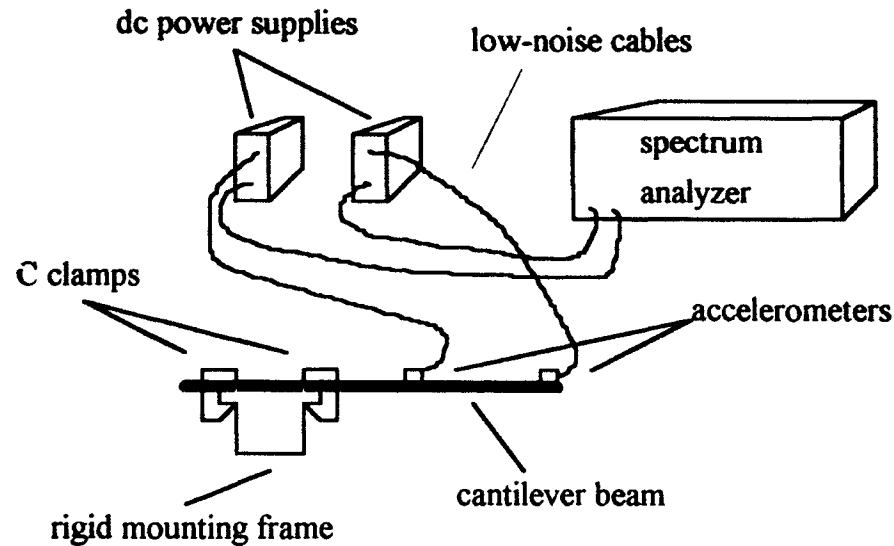


Figure 1. Experimental Set-up

Tapping by the researcher's finger at midspan was the excitation used . This transient excitation covers a range of frequencies, as opposed to just one as in sinusoidal excitation. It was important to see if mode shapes could be obtained using such an excitation because the thin web that eventually will be analyzed must also be excited at many frequencies, in order to achieve flutter. One of the accelerometers was stationary and attached to the free end of the beam. The other one was labeled roving and its signal, $A_1(t)$, took the place of the conventional excitation record that would come from an impact hammer. This experiment will aid in answering four questions concerning the determination of mode shapes:

- Is knowledge of a structure's excitation required?
- Does it matter whether acceleration, velocity, or displacement is measured?
- Must the input and output of an FRF be causal?

- Will phase shifts caused by significant damping present any difficulties?

The Frequency Response Function

The signals, $A_1(t)$ and $A_2(t)$, were processed in the usual manner, via the FFT. The output of the algorithm was chosen to be a magnitude and a phase, for both signals.

Symbolically, one can write

$$H(s) = \frac{A_1(s)}{A_2(s)} \quad (1)$$

where H is the FRF in the complex domain, and $A_1(s)$ and $A_2(s)$ are the Fourier transforms of the accelerometers' time histories. The FRF's magnitudes were generated as the roving signal's FFT magnitude divided by the stationary signal's FFT magnitude. The FRF's phases were generated as the roving signal's FFT phase minus the stationary signal's FFT phase, or

$$|H| = \frac{|A_1(s)|}{|A_2(s)|} \quad (2)$$

and

$$\angle H = \angle A_1(s) - \angle A_2(s) \quad (3)$$

It should be noted that the FRF in Equation (1) is only one of many. What follows is a discussion of some various FRF's and their comparison. Figure 2 on page 7 will be helpful.

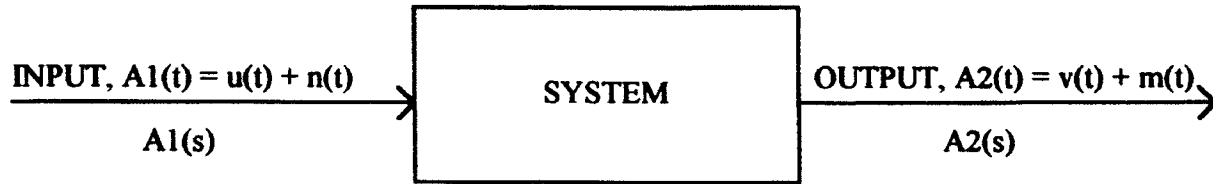


Figure 2. A System to be Analyzed Spectrally

The true input and output are $u(t)$ and $v(t)$, respectively, while $A1(t)$ and $A2(t)$ represent what is measured. The input and output noise are represented by $n(t)$ and $m(t)$, respectively. It is useful to present some definitions here (Harris 1988):

$$G_{A1A1}(s) = A1(s)A1^*(s) \quad (4)$$

$$G_{A2A2}(s) = A2(s)A2^*(s) \quad (5)$$

$$G_{A1A2}(s) = A1(s)A2^*(s) \quad (6)$$

$$G_{A2A1}(s) = A2(s)A1^*(s) \quad (7)$$

In the above equations, G represents an auto spectral density if its subscripts are the same and a cross spectral density if its subscripts are different, while $*$ denotes a conjugate of the Fourier domain's independent variable, s . The following are also true:

$$G_{A1A1}(s) = G_{uu}(s) + G_{nn}(s) \quad (8)$$

$$G_{A2A2}(s) = G_{vv}(s) + G_{mm}(s) \quad (9)$$

The most commonly used FRF is

$$H_1(s) = \frac{G_{A2A1}(s)}{G_{A1A1}(s)} \quad (10)$$

The true frequency response of a system is

$$H_0(s) = \frac{G_{uv}(s)}{G_{uu}(s)} \quad (11)$$

Using Equation (8), it can be shown that

$$H_1(s) = \frac{G_{uv}(s)}{G_{uu}(s) + G_{nn}(s)} = H_0(s) \left(\frac{1}{1 + \frac{G_{nn}(s)}{G_{uu}(s)}} \right) \quad (12)$$

which demonstrates that $H_1(s)$ deviates from $H_0(s)$ due to noise occurring in the input signal (Modal Analysis Theory 1984). Substituting Equations (4) and (7) into Equation (10), one can also show that

$$H_1(s) = \frac{A_2(s)A_1^*(s)}{A_1(s)A_1^*(s)} = \frac{A_2(s)}{A_1(s)} = H(s) \quad (13)$$

which demonstrates that $H_1(s)$ is equivalent to the true frequency response for a noiseless system, since $H(s)$ is equal to $H_0(s)$ when noise is not present.

Another commonly used FRF is (Harris 1988)

$$H_2(s) = \frac{G_{A_2A_2}(s)}{G_{A_1A_2}(s)} \quad (14)$$

Using Equation (9), it can be shown that

$$H_2(s) = H_0(s) \left(1 + \frac{G_{nn}(s)}{G_{vv}(s)} \right) \quad (15)$$

which demonstrates that $H_2(s)$ deviates from $H_0(s)$ due to noise occurring at the output (Modal Analysis Theory 1984). Substituting Equations (5) and (6) into Equation (14), one can show that

$$H_2(s) = \frac{A_2(s)A_2^*(s)}{A_1(s)A_2^*(s)} = \frac{A_2(s)}{A_1(s)} = H(s) \quad (16)$$

which demonstrates that $H_2(s)$ is equivalent to $H_0(s)$ for a noiseless system (Harris 1988).

A newer FRF is

$$H_v(s) = \sqrt{H_1(s)} \sqrt{H_2(s)} \quad (17)$$

Substituting Equations (12) and (15) into Equation (17), one can show that

$$H_v(s) = H_0(s) \sqrt{\left(1 + \frac{G_{mm}(s)}{G_{ww}(s)}\right) / \left(1 + \frac{G_{nn}(s)}{G_{uu}(s)}\right)} \quad (18)$$

thus demonstrating that $H_v(s)$'s accuracy is dependent on input and output noise; however, since this dependency is of the half-order power, $H_v(s)$ is actually more accurate than $H_1(s)$ or $H_2(s)$. Inspection of Equation (18) also clearly shows that $H_v(s)$ is equivalent to the true frequency response for a noiseless system (Modal Analysis Theory 1984).

For the experiment conducted using the cantilever beam, $H_1(s)$ and $H_2(s)$ were plotted. These plots did not result in significant peaks at some of the natural frequencies, thus making them undesirable for the peak picking algorithm later used to determine mode shapes. $H_v(s)$ could not be formulated on the Data Precision 6100 spectrum analyzer because of limited memory. $H(s)$ was ultimately used because noise was not a significant problem in the system and because the resonance peaks were quite obvious in plots of the Fourier transforms of acceleration time histories.

CHAPTER II

FUNCTION OF A MODAL ANALYZER

Spectral Analysis

A modal analyzer encompasses two processing elements, one of which is a spectrum analyzer, or signal processor. The primary function of this unit is to convert time signals into frequency signals. The means by which signal conversion takes place is the Fast Fourier Transform, or FFT. When a time signal is transformed into the frequency domain, the result can be an imaginary part vs. frequency and a real part vs. frequency. Output is most commonly viewed graphically in the form of a magnitude and a phase, both plotted vs. frequency. When a time signal is transformed into a frequency signal, the resulting frequency signal has infinite domain (i.e. the frequency axis extends to positive and negative infinity); therefore, a specified frequency range is chosen by the user. For structural analysis, this range is positive and usually toward the lower end of the frequency spectrum. The available transducers that produce the time signals fed into the analyzer yield an analog signal and often have varying output voltage ranges. For spectral analysis, the FFT must be implemented, which means the signal the FFT algorithm operates on must be a discrete time signal. Therefore, analyzers must have an analog to digital converter. The converter in the modal analyzer used in the experiment discussed in this paper was 8-bit. The varying output voltage of available transducers is accommodated by amplifiers built into the analyzer that can either increase or decrease the voltage range of the signal to be processed.

For modal analysis, an input and an output signal of a structure are usually measured.

These signals could each be any of force, acceleration, velocity, or displacement measurements. Once these signals are converted to the frequency domain, the spectrum analyzer can manipulate them in various ways. For instance, one might divide the magnitude of the output in the frequency domain by the magnitude of the input in the frequency domain and subtract the input's phase angle from the output's phase angle in order to arrive at the transfer function, or frequency response function, between two respective points of measurement. For structural analysis, FRF's are obtained between several points on the structure, with every FRF having its input (or in some cases, its output) be the frequency signal from one particular reference measuring point on the structure. If an input is used as such a reference, the FRF is said to be of inertance type; whereas, if an output is used as the reference, the FRF is labeled mobility type. Other possible results from frequency response manipulation include Nyquist plots and Bode plots. FRF's, however, are the most important results for modal analysis.

Parameter Estimation

The other processing element of a modal analyzer is the modal program, which uses the FRF's obtained from the spectral analysis in order to estimate the parameters of the structure. These parameters may include the modes shapes and the modal mass, stiffness, and damping matrices. The latter three are collectively called the modal model. The Zonic 6088 Modal Analyzer, used in preliminary testing of the beam discussed in this paper, implements three popular parameter estimation techniques: peak picking, circle fit, and multi-degree-of-freedom (mdof) complex exponential curve fit. In the research conducted, only the peak picking technique was used.

Peak picking is the simplest parameter estimation technique. It assumes the structure can be modeled as one or more single degree of freedom systems. The magnitude of the FRF between any two points reaches a local maximum at the resonant frequencies of the structure and approaches zero away from the resonant frequencies. Therefore, every FRF

will consists of several humps always occurring at the same frequencies, which are the structure's resonant frequencies. The differences between the many FRF's lie in the magnitudes of these resonance maxima at the particular resonant frequencies. A mode shape exists for every natural frequency, and for a continuous system, these mode shapes can be approximated by discrete, relative magnitudes at each of the points of measurement. These relative magnitudes are the same as the relative magnitudes of the resonance maxima at one particular frequency, taken from all of the FRF's. It must be noted that, even for a lightly damped structure (a condition that the very use of peak picking assumes), there is a difference between the resonant and the natural frequencies. Therefore, one might question the use of FRF magnitudes at the resonant frequencies when mode shapes are actually associated with natural frequencies. Recall that the FRF's have real and imaginary parts. For an inertance type of FRF, the maxima of the imaginary part occur at the natural frequencies. For the mobility type, the maxima of the real part occur at the natural frequencies. Thus, an apparent dilemma is resolved. The peak picking technique will not, however, generate a modal model.

The next level of sophistication for the single degree of freedom parameter estimation technique is the circle fit. It is better than peak picking because it uses more values around the resonance point than just the peak value. If a frequency shift among the FRF's measured from different locations of the structure occurs, peak picking may miss the peak, but the circle fit will still yield a good result (Modal Analysis Theory 1984).

The mdof complex exponential curve fit is a least square algorithm which uses all of the FRF's simultaneously in order to obtain the global parameters (resonant frequency and damping). Because of the errors in measurement, the resonant frequencies (and damping) may differ from FRF to FRF. One solution would be to average all of the values together, but a better way is to use all FRF's simultaneously (Modal Analysis Theory 1984).

Considerable explanation of both the circle fit and complex exponential curve fit could be provided, but since neither technique was used in the experiment discussed in this

paper, this author deems it unnecessary. Both techniques resolve the modal model, a result not obtainable in the aforementioned experiment because of reasons discussed in the Appendix.

CHAPTER III

THEORETICAL PREDICTIONS

Natural Frequencies

The natural frequencies of a simple structure, such as the cantilever beam used in the experiment discussed in this paper, are easily calculated. The natural frequencies of a cantilever beam have been calculated to be:

$$\omega_r = \lambda_r \left(\frac{EI}{\rho A} \right)^{\frac{1}{2}} \quad r=1, \dots, \infty \quad (19)$$

where E is the elastic modulus, I is the second moment of area, ρ is the density, A is the cross-sectional area, λ is an eigenvalue of the structure, and r is the mode number. The λ 's of the first five modes for a 16 inch beam are (Craig 1981):

$$\lambda_1 = .1172 \text{in}^{-1} \quad (20)$$

$$\lambda_2 = .2934 \text{in}^{-1}$$

$$\lambda_3 = .4909 \text{in}^{-1}$$

$$\lambda_4 = .6873 \text{in}^{-1}$$

$$\lambda_5 = .8836 \text{in}^{-1}$$

The beam used in the experiment has a length of 16 inches, a width of .75 inches, a height of .1 inches, an elastic modulus of 29×10^6 psi, a second moment of area of 6.25×10^{-5}

in⁴, a density of .3 lb/in³, and a cross-sectional area of .075 in². The elastic modulus and density are assumed values based on the fact that the beam is comprised of steel, and were not actually measured. Equation (19) yields a result in radians/sec, but division by 2π yields the first five natural frequencies in Hertz:

$$f_1 = 12.1954 \quad (21)$$

$$f_2 = 76.411$$

$$f_3 = 214.008$$

$$f_4 = 419.388$$

$$f_5 = 693.220$$

Mode Shapes

A general equation for the mode shapes of a cantilever beam has also been derived:

$$V_r(x) = C \{ \cosh(\lambda_r x) - \cos(\lambda_r x) - k_r [\sinh(\lambda_r x) - \sin(\lambda_r x)] \} \quad (22)$$

where C is an arbitrary constant, x is the horizontal location on the beam in inches and is equal to zero at the clamped end of the beam, and k_r takes on the following dimensionless values for the first five modes of a 16 inch beam (Craig 1981):

$$k_1 = .7341 \quad (23)$$

$$k_2 = 1.019$$

$$k_3 = .9992$$

$$k_4 = 1$$

$$k_5 = 1$$

CHAPTER IV

RESULTS

Preliminaries

The natural frequencies of the beam were the first things sought after. These frequencies were determined roughly by moving the roving accelerometer along the beam and measuring FRF's between it and the stationary accelerometer. Only the magnitude was plotted, and these graphs had obvious peaks at the resonant frequencies. During these preliminary measurements, a Zonic 6088 modal analyzer was used to collect the data. A typical time signal from one of the accelerometers looks like Figure 3 on page 17. When converted to the frequency domain, this signal has a corresponding magnitude and phase plot shown in Figure 4 on page 18. As can be seen in the magnitude plot on top, the resonant peaks are very obvious, and since the structure under consideration is very lightly damped (virtually all of its damping comes from the clamps used to approximate an ideal, fixed end), these frequencies may be considered to be the natural frequencies. The numbers written on the phase plot on the bottom indicate the phases at the natural frequencies. Table 1 on page 19 shows the ranges of the natural frequencies obtained from all sixteen of the FRF's measured. The theoretical natural frequencies of Equations (21) are repeated in this table for comparison.

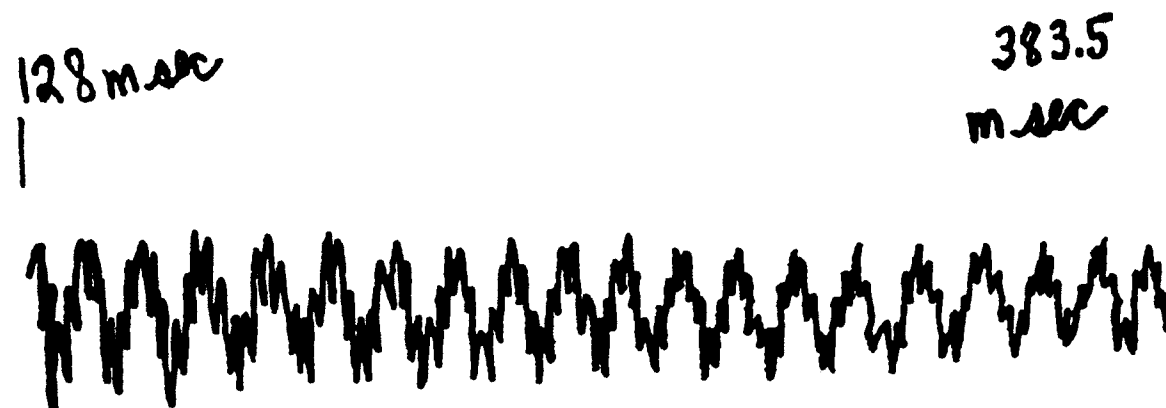


Figure 3. Typical Time Signal from an Accelerometer
(traced by hand from screen)

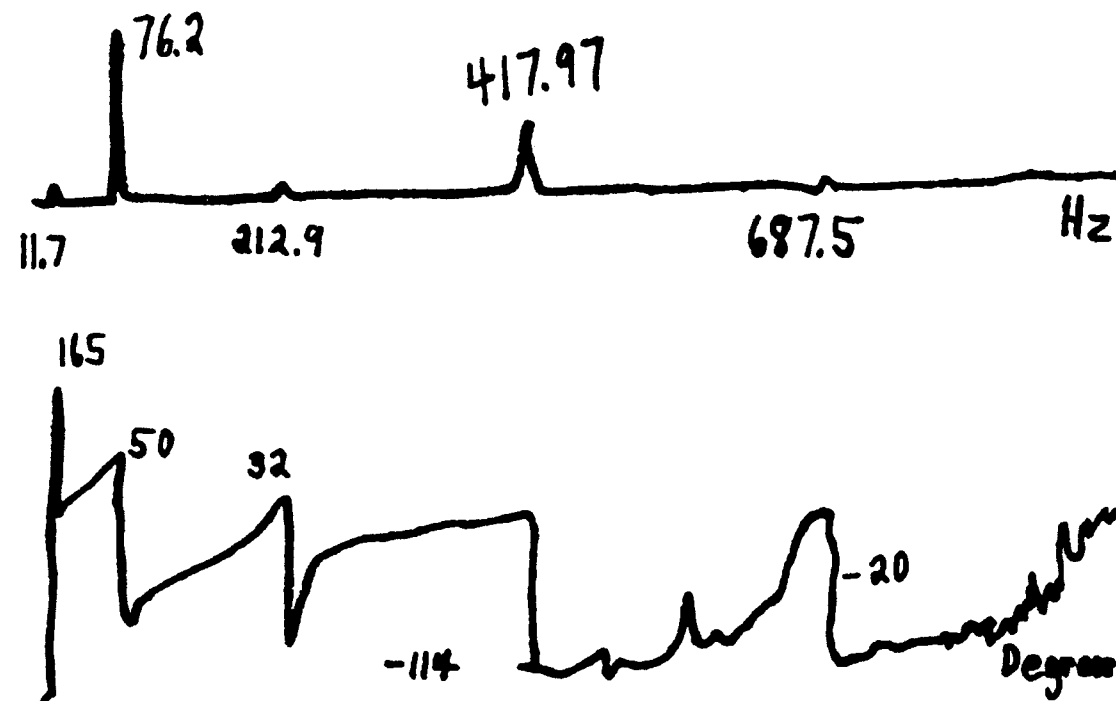


Figure 4. FFT Magnitude and Phase Plots for Signal in Figure 3 on Page 17
(traced by hand from screen)

TABLE 1
RANGES OF MEASURED NATURAL FREQUENCIES

Mode Number	Measured Range (Hertz)	Theoretical natural frequency (Hertz)
1	11.719 only	12.1954
2	76.172 only	76.4119
3	208.984 to 214.843	214.008
4	414.062 to 419.921	419.388
5	687.5 to 695.312	693.220

Finding the Mode Shapes

The data-taking conditions chosen on the spectrum analyzer were 1024 (a power of two is necessary so that the FFT can be taken) points of measurement (or samples), a 500 microsecond sample period, a 128 millisecond delay (because the initial time history is somewhat erratic and may get cut-off at the top and bottom due to too much voltage coming in), and no windowing. Sixteen stations where acceleration would be measured were marked off at one inch intervals along the beam. The experiment was also repeated to check for consistency of results, and, indeed, they were consistent.

The sixteen FRF's had as their reference point the Fourier transform of the signal produced by the stationary accelerometer located at the free end of the beam. A typical FRF magnitude plot looks like the top of Figure 5 on page 21. At first glance, this plot may seem strange because the natural frequencies are not apparent as they are in

magnitude plots of FFT's of accelerometer signals. Upon further reflection, however, the FRF magnitude plots do make sense because they are the division of two signals that are very similar--both signals peak in the same locations and are flat in the same regions--and, hence, should approach unity for all frequencies. Although the variation from unity is slight, it can be measured with great precision due to the 14-bit resolution of the Data Precision 6100. Hilly regions usually occur due to anomalies in one of the FFT magnitude plots used to create the FRF magnitude plot; i.e., if one plot isn't quite flat at antiresonance and the other plot is flat at this frequency, then the division of the two will create a hilly region around that frequency. The hilly regions were not investigated any further because only the values of the FRF magnitude plots at resonance were used in the determination of mode shapes. A typical FRF phase plot looks like the bottom of Figure 5 on page 21. The numbers on this plot indicate the phase at the natural frequencies. The phase is used to govern the sign of the magnitude read off at the natural frequencies, and it was always near either 0 or 180 degrees at resonance, as it should be for a lightly damped structure. Without the phase plot, all magnitude values would be positive, and that would make it impossible to get mode shapes higher than the first mode because the higher modes have nodes, or points of crossover between positive and negative relative deflection. Of course, the scaling of a mode shape is arbitrary, so a magnitude may be labeled positive for a corresponding phase of 180 degrees as long as the magnitudes with 0 degree phase are labeled negative, or vice versa.

Given the arbitrary scaling of the mode shapes, the plots of Equation (22) and the measured modes have been scaled so that they have one point of identical value and plotted in Figures 6 through 10 on pages 22 through 26. Having one point of identical value (set equal to positive or negative unity) allows one to compare the measured vs. the theoretical values at the other locations along the beam. Table 2 on page 27 is a listing of the measured values of relative deflection vs. the theoretical relative deflections for the first five modes at the sixteen stations of measurement.

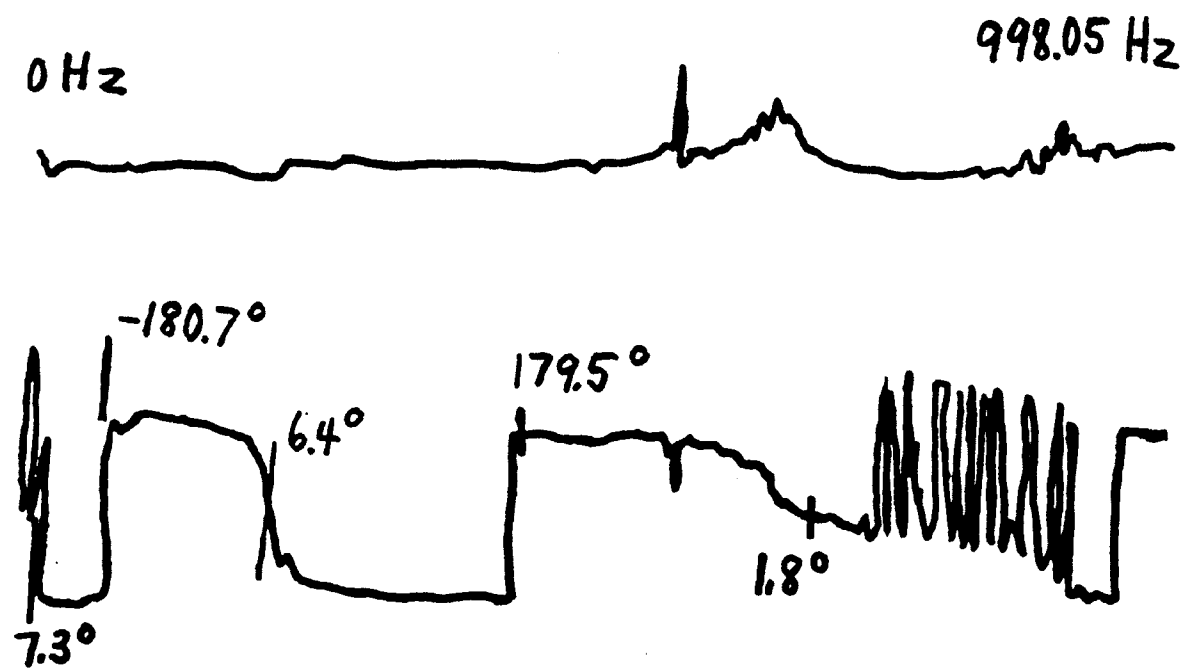


Figure 5. Typical FRF Magnitude and Phase Plots
(traced by hand from screen)

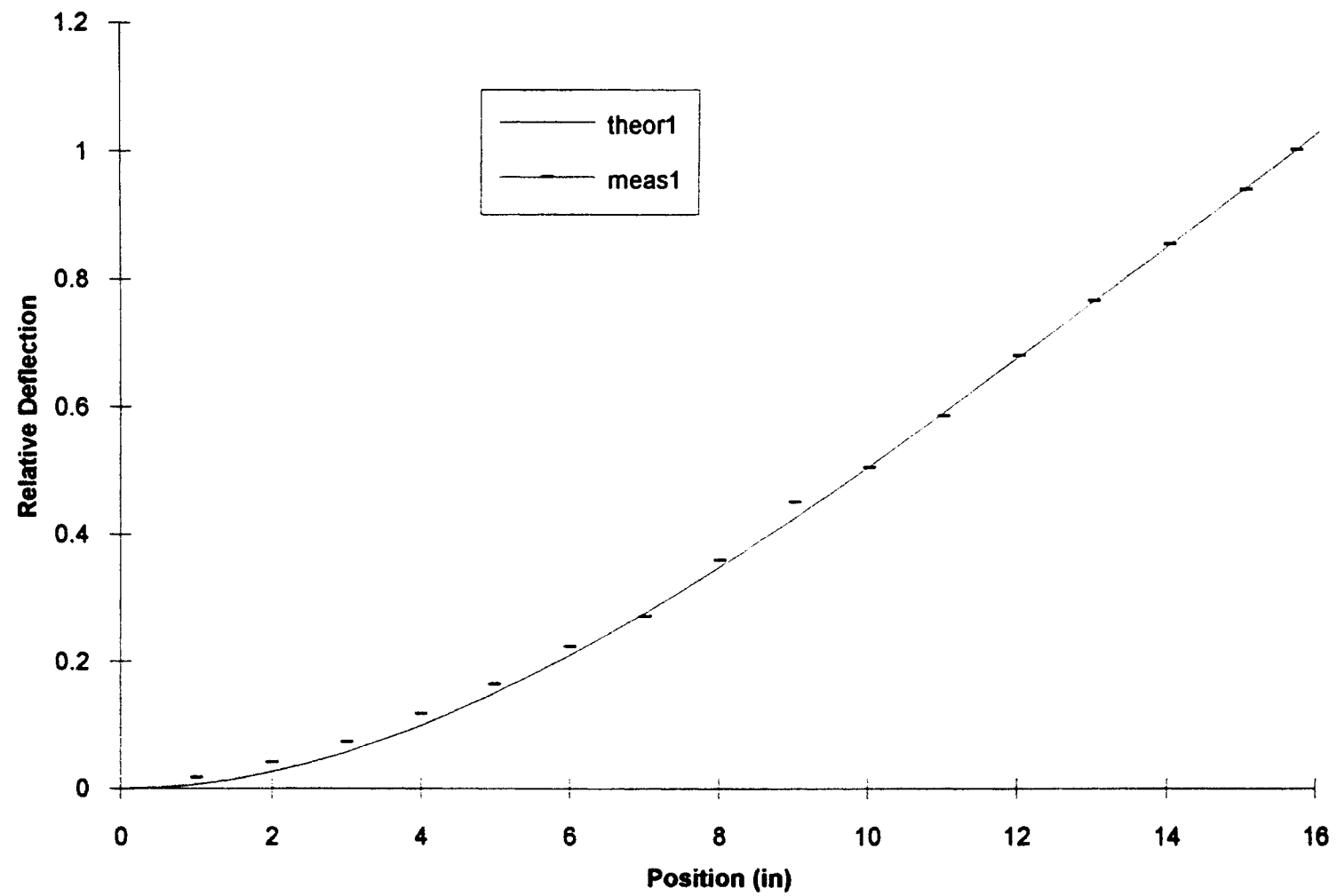


Figure 6. Measured vs. Theoretical for First Mode

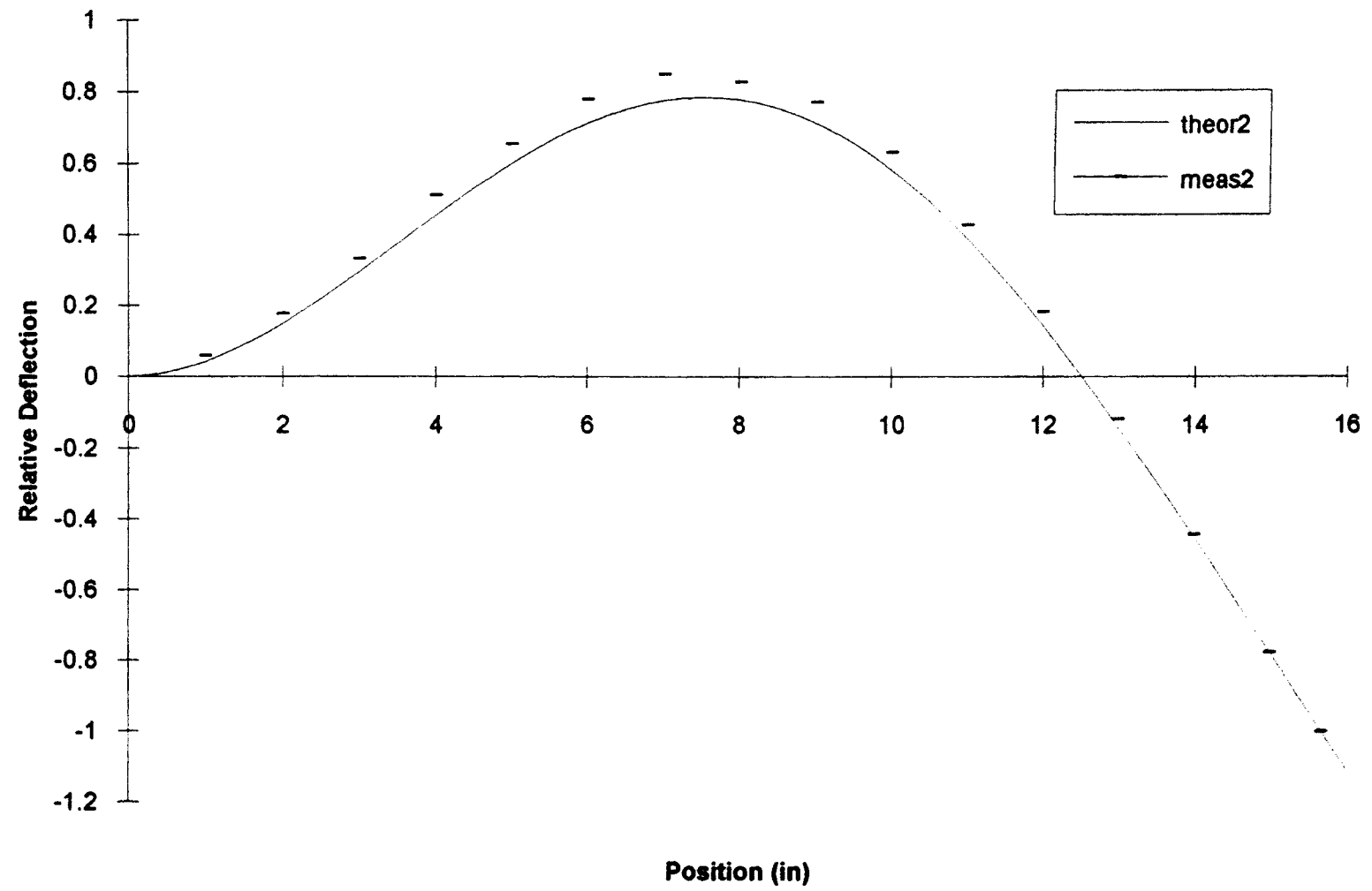


Figure 7. Measured vs. Theoretical for Second Mode

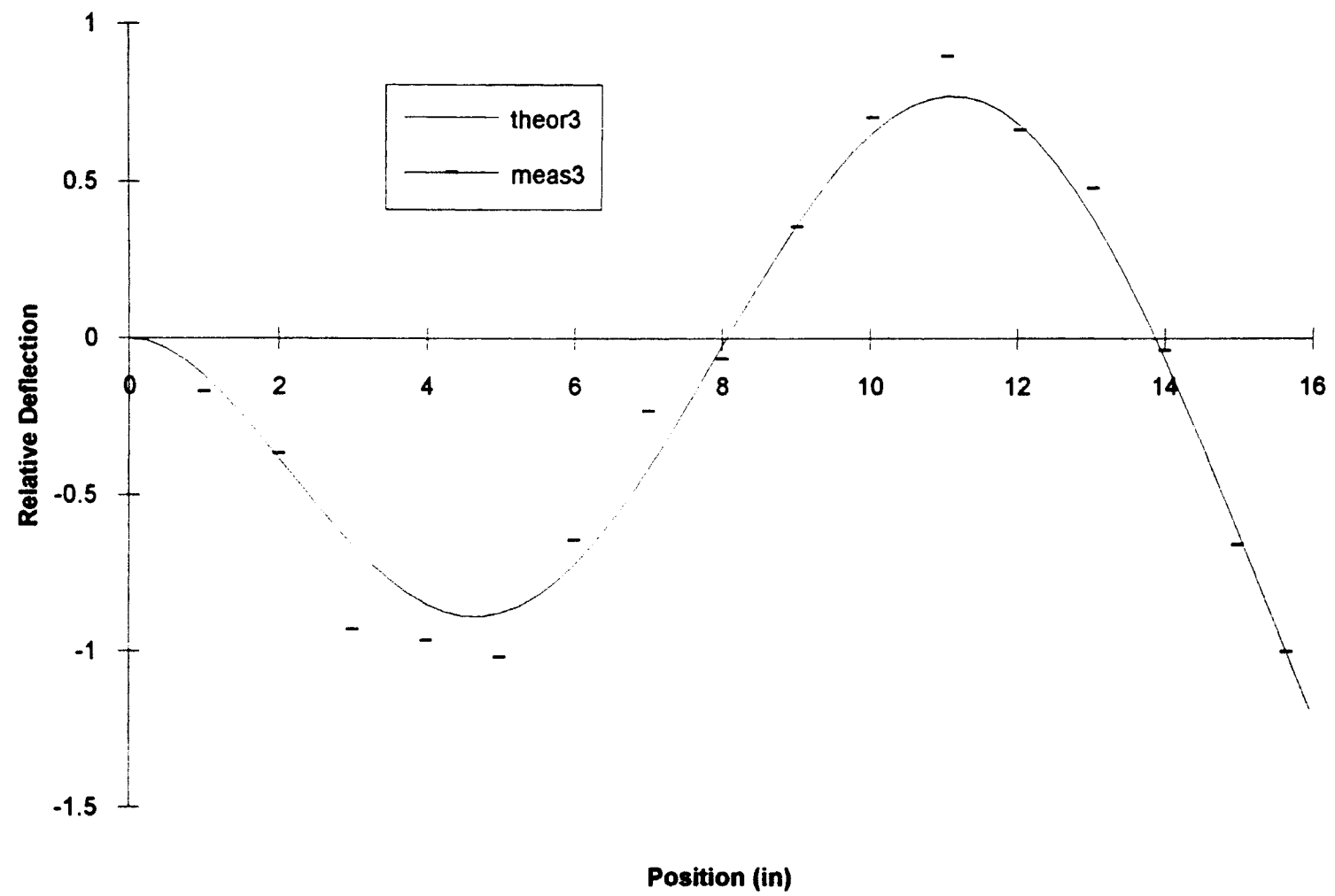


Figure 8. Measured vs. Theoretical for Third Mode

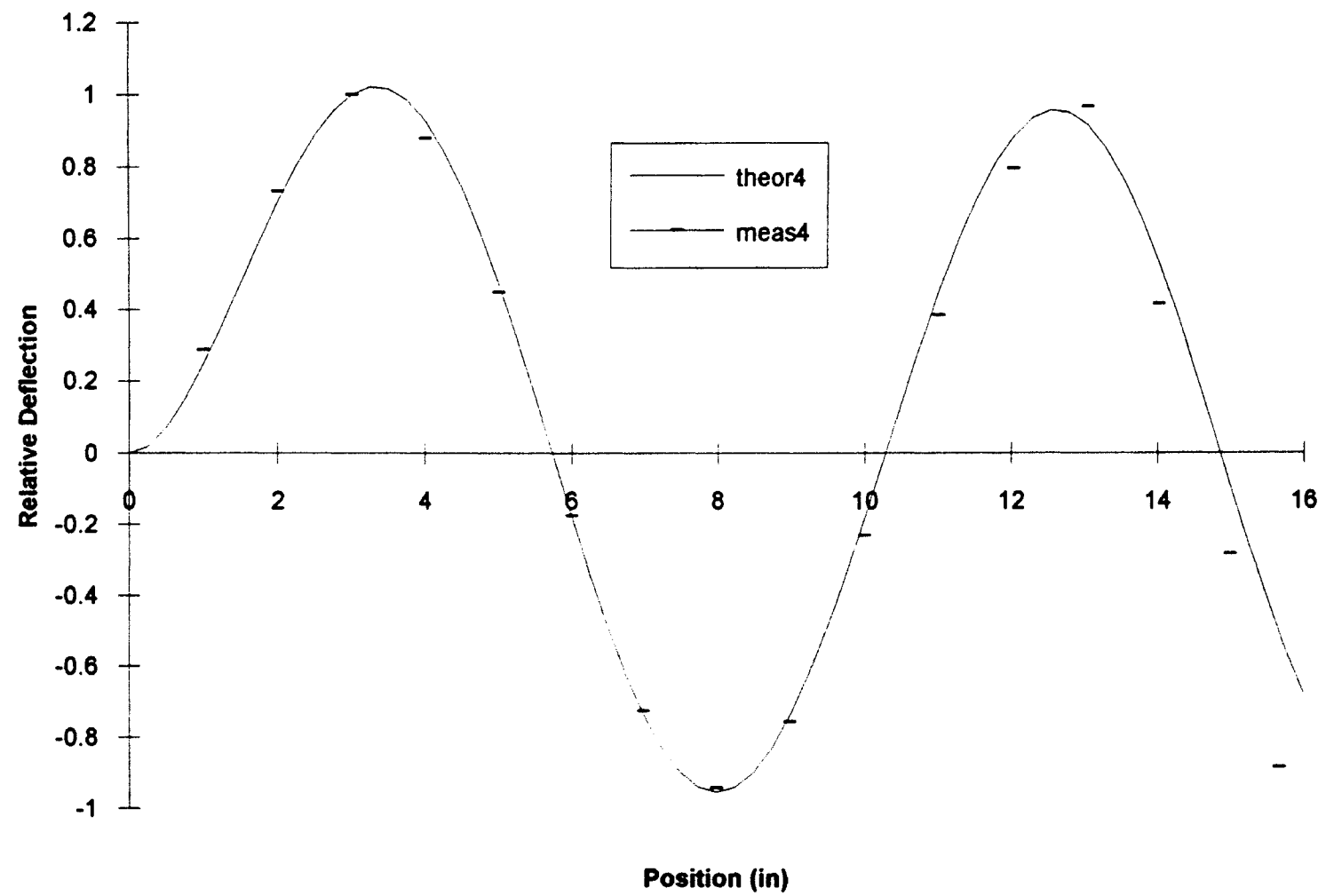


Figure 9. Measured vs. Theoretical for Fourth Mode

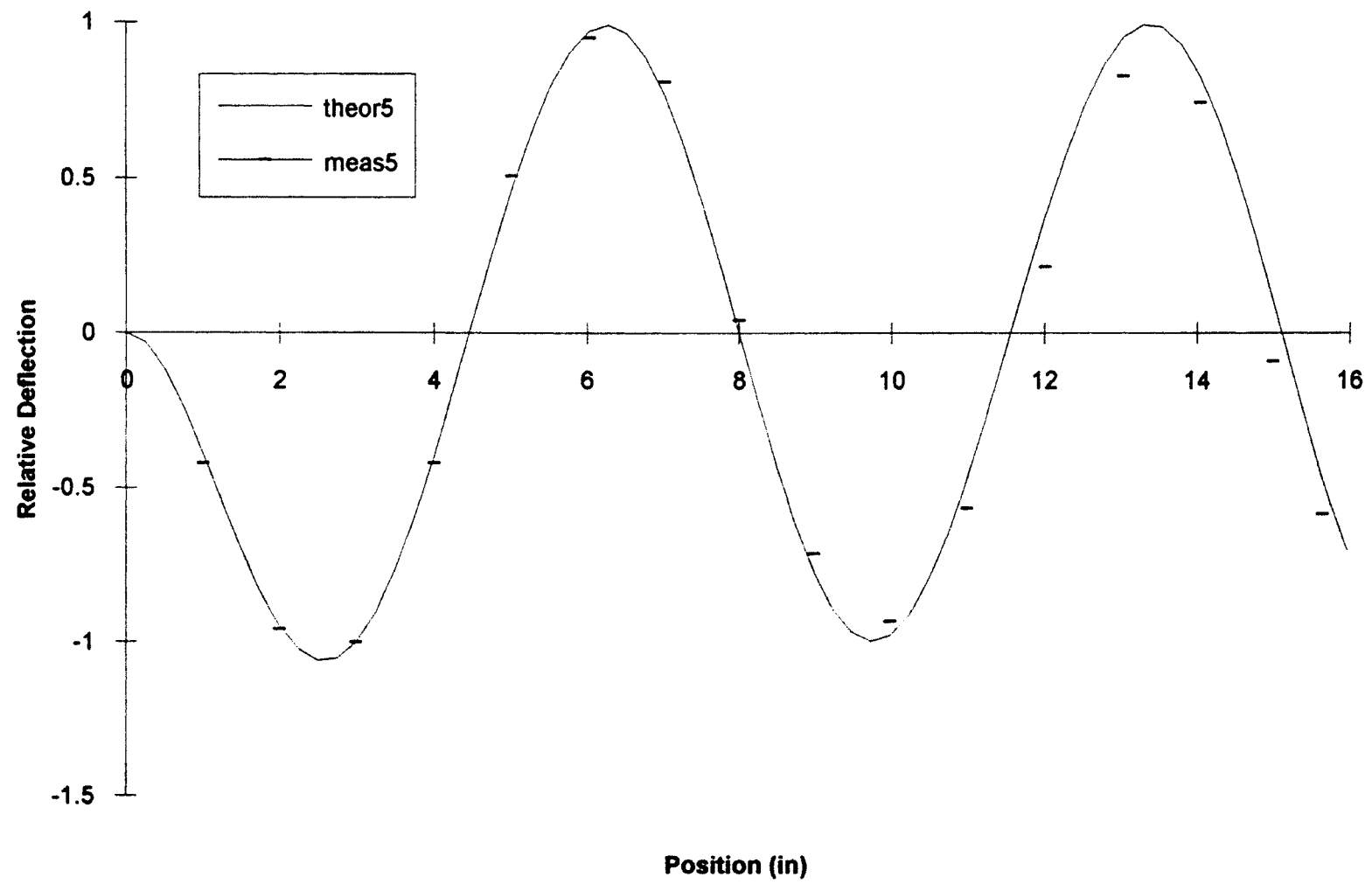


Figure 10. Measured vs. Theoretical for Fifth Mode

TABLE 2

MEASURED VS. THEORETICAL MODE SHAPES

x	theor1	meas1	theor2	meas2	theor3	meas3	theor4	meas4	theor5	meas5
1	0.006862	0.01731	0.042275	0.05777	-0.11809	-0.17063	0.246128	0.288893	-0.38764	-0.42082
2	0.026639	0.0418	0.150434	0.17614	-0.3812	-0.36592	0.701607	0.731489	-0.94582	-0.95779
3	0.058117	0.07321	0.296851	0.33404	-0.66032	-0.92909	1	1	-1	-1
4	0.100087	0.11872	0.455059	0.511256	-0.84868	-0.96411	0.92554	0.879324	-0.40048	-0.41852
5	0.151352	0.16522	0.600807	0.655231	-0.87702	-1.01545	0.471663	0.448118	0.459847	0.506842
6	0.210735	0.22409	0.713198	0.778749	-0.72377	-0.64203	-0.17584	-0.17501	0.970659	0.948582
7	0.277086	0.27157	0.77575	0.849326	-0.41658	-0.23168	-0.73317	-0.72216	0.766197	0.808643
8	0.349296	0.36012	0.777202	0.827879	-0.02358	-0.06535	-0.95238	-0.94086	-0.00081	0.040929
9	0.426309	0.45065	0.711966	0.77104	0.363687	0.35541	-0.73653	-0.75506	-0.76816	-0.71054
10	0.507133	0.50556	0.580132	0.631633	0.652293	0.7025	-0.18492	-0.23201	-0.97418	-0.92876
11	0.59086	0.5857	0.386983	0.42681	0.769454	0.8948	0.451315	0.38359	-0.46798	-0.56415
12	0.676673	0.6787	0.142025	0.1823	0.678607	0.66296	0.882953	0.794883	0.380366	0.214881
13	0.763872	0.76416	-0.14243	-0.11755	0.385859	0.47855	0.913831	0.964834	0.950539	0.824758
14	0.85188	0.853321	-0.45307	-0.44236	-0.06523	-0.03735	0.529844	0.41449	0.825613	0.740858
15	0.940268	0.937298	-0.77768	-0.77587	-0.61024	-0.6564	-0.09469	-0.28343	0.096949	-0.09107
15.675	1	1	-1	-1	-1	-1	-0.50998	-0.88252	-0.475	-0.58378

CHAPTER V

VERIFICATION

Time Response at Free End

Empirically, one surmises that the time response near the beam's base (near the clamped end) must be dominated more by the higher modes than the time response near the free end of the beam is governed by these higher modes. Such a conclusion can be made by observing the differences in FFT magnitude plots corresponding to the free end and the clamped end. For both cases, the lower modes have much larger resonance peaks than the higher modes; however, this disparity is less at the clamped end. Due to this fact, a good check of the acceleration time history obtained at the free end of the beam can be made. Since this time history will depend much more on the lower modes than the higher modes, one can determine a theoretical time history based on the first five modes and compare it to the measured record at the free end. This theoretical record should closely approximate the time history obtained by measurement, since the measured record should depend much more on the first five modes than any higher modes.

It is known that

$$y(x, t) = \sum_{r=1}^{\infty} V_r(x) \frac{1}{\omega_r} \int_0^t Q_r(\tau) \sin \omega_r(t - \tau) d\tau \quad (23)$$

for zero initial velocity and displacement, where

$$Q_r(t) = \int_0^L f(x,t) V_r(x) dx \quad (24)$$

and y is the vertical displacement of the beam in inches, t is time in seconds, f is the external excitation of the beam in pounds, and L is the length of the beam in inches (Meirovitch 1986). In applying the aforementioned assumption that the response, y , depends mostly on the lower modes, one can write

$$y(x,t) = \sum_{r=1}^5 V_r(x) \frac{1}{\omega_r} \int_0^t Q_r(\tau) \sin \omega_r(t - \tau) d\tau \quad (25)$$

For the experiment performed, the beam was tapped quickly by the researcher's finger at midspan, or $x = 8$ inches, in order to approximate an impulse imparted to the structure at that point. Therefore,

$$f(x,t) = F\delta(t)\delta(x - 8) \quad (26)$$

where δ represents a unit impulse function and F is the force in pounds imparted to the structure. Knowing Equation (24) allows one to calculate five Q 's corresponding to each of the first five modes, and with the first five natural frequencies already calculated, one can substitute into Equation (25) and obtain the vertical response of the beam used in the experiment:

$$\begin{aligned} y(x,t) = F\{ & .00871 V_1(x) \sin 76.626t \\ & + .00292 V_2(x) \sin 480.11t \\ & + .000029 V_3(x) \sin 1344.6t \\ & - .000526 V_4(x) \sin 2635.1t \\ & + (2.62 \times 10^{-7}) V_5(x) \sin 4355.6t \} \end{aligned} \quad (27)$$

This response is a deflection curve and it can be differentiated twice with respect to time in

order to yield an acceleration curve. When x is set equal to 15.875 inches (the horizontal distance from the clamped end of the center of the accelerometer as it sits on the free end of the beam), the acceleration of the free end of the beam can be calculated to be:

$$\begin{aligned}\ddot{y}(15.875, t) = F\{ & -102.92\sin 76.626t \\ & + 1338.0\sin 480.11t \\ & - 101.66\sin 1344.6t \\ & - 3387.1\sin 2635.1t \\ & - 4.4700\sin 4355.6t\} \end{aligned} \quad (28)$$

This acceleration curve is plotted in Figure 11 on page 31. At first glance, one may think that only two modes are being represented since the plots seem to represent the summation of only two sine waves. In actuality, however, all five terms of Equation (28) are represented. The most predominant terms are the second and fourth due to their relatively large amplitudes and they appear quite readily. The first term is barely noticeable because its period is very long--two thirds the length of the figure. The fifth term has such a small amplitude and period that it is not resolved in the figure. The third term has a period almost exactly twice that of the fourth term and, therefore, merely adds some asymmetry to the waves produced by the latter. Figure 12 on page 32 is a plot of the measured acceleration curve at the free end of the beam. The theoretical curve has been scaled for comparison to the measured curve so that both plots cover the same period of time. One can see that the curves are quite similar, and hence, that theory compares closely with reality. The closeness of the comparison is a verification that acceleration is being measured accurately by the transducer.

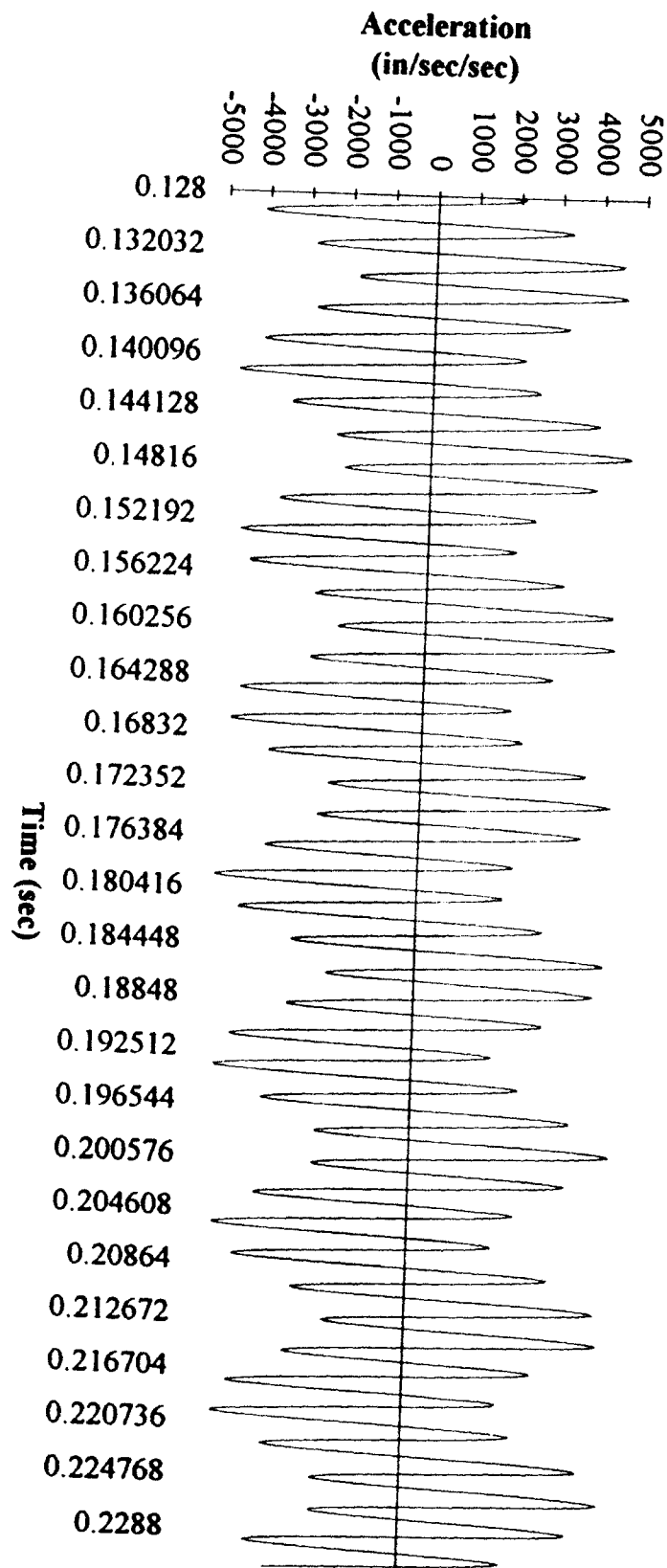


Figure 11. Theoretical Acceleration of the Beam's Free End

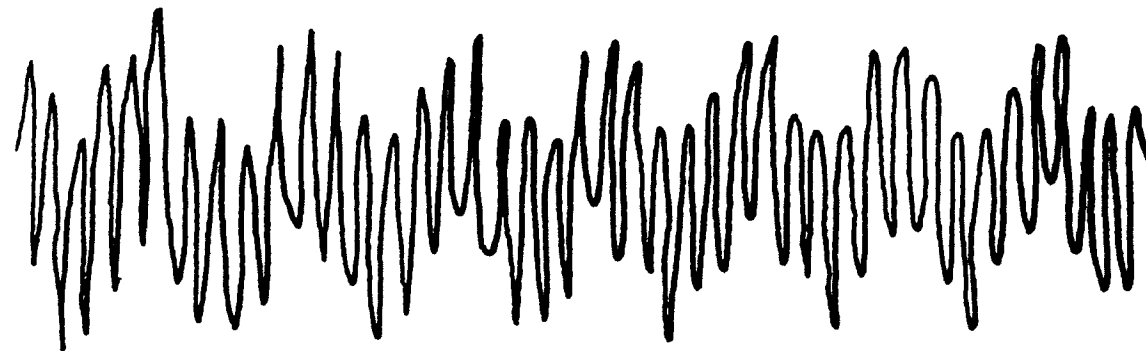


Figure 12. Measured Record from Free End Accelerometer
(traced by hand from screen)

Modal Assurance Criterion

One of the means by which modal analysts can become confident of their results is to test the modal assurance criterion, or MAC. This criterion suggests that orthogonality or near orthogonality of the measured modes means that they are very close to the actual modes of the structure tested. One can determine whether or not the measured modes are normal or not by placing them into a matrix as column vectors and then attempting to diagonalize this matrix. The closer one can get to 1's along the diagonal and 0's elsewhere, the more one can be assured of having found the normal modes of the structure (Modal Analysis Theory 1984). The matrix having as columns the measured modes obtained in the experiment is

$$\begin{bmatrix}
 0.01731 & 0.05777 & -0.17063 & 0.288893 & -0.42082 \\
 0.0418 & 0.17614 & -0.36592 & 0.731489 & -0.95779 \\
 0.07321 & 0.33404 & -0.92909 & 1 & -1 \\
 0.11872 & 0.511256 & -0.96411 & 0.879324 & -0.41852 \\
 0.16522 & 0.655231 & -1.01545 & 0.448118 & 0.506842 \\
 0.22409 & 0.778749 & -0.64203 & -0.17501 & 0.948582 \\
 0.27157 & 0.849326 & -0.23168 & -0.72216 & 0.808643 \\
 0.36012 & 0.827879 & -0.06535 & -0.94086 & 0.040929 \\
 0.45065 & 0.77104 & 0.35541 & -0.75506 & -0.71054 \\
 0.50556 & 0.631633 & 0.7025 & -0.23201 & -0.92876 \\
 0.5857 & 0.42681 & 0.8948 & 0.38359 & -0.56415 \\
 0.6787 & 0.1823 & 0.66296 & 0.794883 & 0.214881 \\
 0.76416 & -0.11755 & 0.47855 & 0.964834 & 0.824758 \\
 0.853321 & -0.44236 & -0.03735 & 0.41449 & 0.740858 \\
 0.937298 & -0.77587 & -0.6564 & -0.28343 & -0.09107 \\
 1 & -1 & -1 & -0.88252 & -0.58378
 \end{bmatrix}$$

(29)

When one attempts to diagonalize this matrix, one obtains

```

1 0 0 0 0
0 1 0 0 0
0 0 1 0 0
0 0 0 1 0
0 0 0 0 1
0 0 0 0 0
0 0 0 0 0
0 0 0 0 0
0 0 0 0 0
0 0 0 0 0
0 0 0 0 0
0 0 0 0 0
0 0 0 0 0
0 0 0 0 0
0 0 0 0 0
0 0 0 0 0
0 0 0 0 0
0 0 0 0 0

```

(30)

which demonstrates that the obtained vectors are linearly independent. One is thus assured that normal modes have been obtained.

CHAPTER VI

CONCLUSION

The hypothesis that mode shapes could be obtained by exciting a structure with an unknown transient and measuring only accelerations was confirmed. The research conducted shows that when attempting to find mode shapes:

- Knowledge of the excitation is not necessary
- The vibrations measured do not have to be accelerations; they may be velocities or even displacements
- Causality between input and output is not required

One might question exactly how unknown the excitation was, since it was chosen to approximate an ideal impulse; however, not only were its magnitude and duration unknown (and, hence, not used in the determination of the mode shapes), but any transient excitation could have been used. As stated earlier, an impulse was chosen so that the higher frequencies could be excited. Had some other form of excitation been chosen--one corresponding to a more constrained frequency band--then the modes associated with natural frequencies within this band would have been excited much more than the others, making the others difficult to determine. In fact, when this researcher failed to tap the beam quickly enough (i.e., the impulse had greater duration and thus excited a lower frequency range), the fifth mode became very difficult to determine because the FFT

magnitude plots of the accelerometer signals had no appreciable peak beyond the fourth natural frequency. Without a noticeable peak, the peak picking method could not be applied effectively. And so, the chosen form of excitation was merely used to excite the modes of interest, not because knowledge of this excitation is required to find the mode shapes.

In the case of the thin polymer web eventually to be analyzed, vibration can only be measured in the form of velocity. The question was posed, in the introduction, as to whether or not it would make a difference if velocity were measured, as opposed to acceleration. One might suggest that these velocities be differentiated into accelerations, and then manipulated as in the experiment discussed in this paper. This procedure would certainly be valid, but the step of differentiation is unnecessary, and undesirable because it may introduce errors. A simpler and more accurate method would be to obtain FRF's from the Fourier transforms of velocity signals, instead of accelerometer signals. These Fourier transform magnitudes will only differ from Fourier transform magnitudes obtained from acceleration time histories by a constant. This constant happens to be the frequency, ω . Since all magnitude plots will be divided by the same constant at all frequencies, the resulting FRF's would be the same as those one would obtain using accelerations. The same procedure could also be followed using displacement measurements. Of course, if the FRF's are the same for all three cases, then the modes they yield must be the same.

Another issue brought up in the introduction was that of causality, or whether it would matter which accelerometer was affected by the excitation first. Either signal can be used as the trigger to begin the recording of data. In fact, FRF's were obtained using both accelerometers as the trigger for several trial runs. Sometimes, the trigger accelerometer

was located farther away from the point of excitation than the other transducer, resulting in the output being affected before the input. This scenario posed no problem; therefore, causality is not an issue when finding mode shapes using only vibration signals.

CHAPTER VII

SUGGESTIONS FOR FURTHER RESEARCH

The success of this experiment makes one wonder about future experiments that may expand the realm of modal analysis yet further. The structure chosen for the current analysis was a simple cantilever beam with very little damping. The determination of its mode shapes was achieved via the peak picking method. This method, as described earlier, is only reliable for such lightly damped structures. It is known that higher values of damping tend to bring the phase angle at resonance away from its undamped norm of either 0 or 180 degrees. When this phase migration occurs, the peak picking technique becomes useless. The circle fit algorithm, however, could be used to investigate a structure with higher damping. For such an experiment, a modal analyzer must be used because a spectrum analyzer does not have any built-in modal software, i.e., parameter estimation programs. Clearly, if accurate mode shapes are determined for a significantly damped structure excited by an unknown excitation covering a broad frequency range, then analysis of the thin web structures mentioned earlier can begin. Of course, the method of excitation will have to be changed--a tapping of the finger will no longer be satisfactory. Perhaps a continuous cross wind would set the web into flutter vibration that could be detected by laser velocimeters.

WORKS CITED

Craig, Roy R. Jr. 1981. *Structural Dynamics An Introduction to Computer Methods*.

New York: John Wiley & Sons

Harris, Cyril M. 1988. *Shock & Vibration Handbook*. St. Louis: McGraw-Hill

Laura, P.A.A., Pombo, J.L., Susemihl, E.A. 1974. A Note on the Vibrations of a

Clamped Free Beam with a Mass at the Free End. *J. Sound Vib.* 37: 161-168

Meirovitch, Leonard. 1986. *Elements of Vibration Analysis*. San Francisco: McGraw-Hill

Modal Analysis Theory. In *6088 Multichannel Signal Processor Zonic Modal Software*

User Manual. Milford, Ohio: Zonic Corporation, 1984

APPENDIX

OBTAINING A MODAL MODEL WITHOUT MEASURING THE STRUCTURE'S EXCITATION: AN UNDERDETERMINED SYSTEM

One of the requirements for conducting modal analysis is to obtain FRF's between several different measurement points on a structure. The Zonic 6088, used in the preliminaries of the experiment discussed in this paper, requires force vs. acceleration, force vs. velocity, or force vs. displacement FRF's in order to resolve the modal model. In using any of these options, one thing is always true: the input force to the structure must be known. The reason this input force must be known is because the circle fit and the mdof complex exponential curve fit algorithms require it in order to be able to find the modal model. For simplification, let us consider a structure having only two measurement points, the time signals of which are called $y(t)$ and $u(t)$. The signals obtained at these two points are any combination of acceleration, velocity, or displacement; however, neither signal represents the force used to excite the structure. If different types of signals are measured at the two points, one of them can easily be integrated or differentiated in order to make it the same type of signal as measured at the other point. In this, the simplest possible scenario for conducting a theoretical modal analysis, the setup would look as is shown in Figure 13 on Page 42.

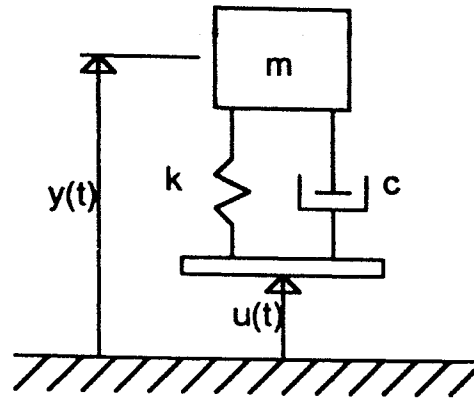


Figure 13. Simplest Modal Analysis Scenario

The symbols k , c , and m represent the stiffness, damping, and mass, respectively, between the two measurement points. The bottom of the figure represents an infinitely rigid ground. The equation of motion for this simple structure is

$$m\ddot{y} + c(\dot{y} - \dot{u}) + k(y - u) = 0 \quad (31)$$

Rearranging the equation yields

$$m\ddot{y} + c\dot{y} + ky = c\dot{u} + ku \quad (32)$$

where the right hand side must be the external forcing function at the location where $y(t)$ is measured. One already knows $u(t)$, and \dot{u} is easily obtained by differentiation of $u(t)$, and $\int_0^t u(\tau)d\tau$ is easily obtained by integrating signal $u(t)$ (it may be necessary to obtain this integral or derivative, depending on what type of signal u is when it's measured--displacement, velocity, or acceleration); therefore, one would only have to know c and k in order to provide the Zonic 6088 with an acceptable FRF with which to perform parameter estimation. The problem is that c and k are not known beforehand; in fact, c

and k are two of the parameters that the modal program tries to find. Consequently, if one does not have a recorded signal of the external excitation to the structure, one would have to know the modal model before one tries to find it!

VITA 2

Peter Martin

Candidate for the Degree of

Master of Science

Thesis: EXPERIMENTAL DETERMINATION OF MODE SHAPES FOR A LIGHTLY DAMPED STRUCTURE WITH UNKNOWN TRANSIENT EXCITATION

Major Field: Mechanical Engineering

Biographical:

Personal Data: Born in Chicago, Illinois, May 24, 1969, the son of Adolf H. and Irmtraut M. Martin.

Education: Graduated from Glenbrook South High School, Glenview, Illinois, in June 1987; received Bachelor of Science Degree in Engineering from Harvey Mudd College in May, 1991; completed requirements for the Master of Science Degree at Oklahoma State University in May, 1994.

Professional Experience: Research Assistant, Department of Mechanical and Aerospace Engineering, Oklahoma State University, June, 1993, to December, 1993.

Team Leader and Member, Aerojet Electronics Systems Division, Azusa, CA, September, 1990, to May, 1991.

Research Assistant, Engineering Department, Harvey Mudd College, June, 1990, to September, 1990.

Team Member, McDonnell Douglas, Huntington Beach, CA, September, 1989, to December, 1989.

Engineering Aide, Adams Elevator Equipment Company, Skokie, IL, June, 1989, to August, 1989.